Roles of inducible nitric oxide synthase in the development and healing of experimentally induced gastric ulcers

MASAYUKI TATEMICHI*[†], TSUTOMU OGURA[†], NOBUYUKI SAKURAZAWA[†], HIROSHI NAGATA[‡], MINORU SUGITA* AND HIROYASU ESUMI[†]

*Department of Environmental and Occupational Health, Toho University School of Medicine, Tokyo, Japan, [†] Investigative Treatment Division, National Cancer Center Research Institute, East, Chiba, Japan, and [‡] Department of Internal medicine, Keio University School of Medicine, Tokyo, Japan

Summary. The roles of inducible nitric oxide synthase (iNOS) in the development and healing of gastric ulcers have not been fully characterized. We characterized iNOS expression in experimentally induced ulcers in rat and mouse stomachs and investigated the roles of iNOS using iNOS gene-deficient (iNOS$^{-/-}$) mice and wildtype mice. Gastric ulcers were induced in rats and mice by the application of acetic acid and cryoinjury, respectively. iNOS expression was detected on days 1–7 and peaked 3 days after ulcer induction in the rat. iNOS-positive cells were distributed mainly among the infiltrating cells and fibroblasts in the ulcer bed. The almost similar courses of healing and iNOS expression were observed in the ulcers of mice. During the course of healing, the iNOS gene status did not affect cell proliferation in the healing zone or vessel formation in the ulcer bed. iNOS deficiency, however, caused larger ulcers and severer inflammation during ulcer healing; the clearance of inflammatory cells in the ulcer bed by apoptosis was also delayed when the ulcer was re-epithelialized in the iNOS-deficient mice. These results indicate that iNOS is expressed in the ulcer bed and that iNOS activity may play beneficial roles in the ulcer repair process, possibly by regulating inflammation.

Keywords: expression, gastric ulcer, inflammation, iNOS

Correspondence: Masayuki Tatemichi, MD, Department of Environmental and Occupational Health, Toho University School of Medicine, 5-21-16, Omori-nishi, Ota-ku, Tokyo 143-8540, Japan. Tel.: +81 3 3762 4151; Fax: +81 3 5493 5416; E-mail: tatemich@med.toho-u.ac.jp

Nitric oxide (NO) has been shown to protect the gastro-intestinal mucosa from a variety of insults, including caustic injuries from ethanol, mineral acids and bile-acids, ischaemia/reperfusion injuries and early

endotoxin-induced damage (Salzman *et al.* 1998). The main roles of NO are thought to be the maintenance of microcirculation homeostasis in the mucosa and the inhibition of inflammatory neutrophil accumulation via the downregulation of the surface expression of adhesion molecules (Kubes *et al.* 1991). However, whether NO produced by inducible nitric oxide synthase (iNOS) exerts beneficial or detrimental effects on gastrointestinal mucosal integrity is still a topic of debate. iNOS activity is known to exert an anti-inflammatory effect on intestinal inflammation (McCafferty *et al.* 1997). Peroxynitrites produced by the chemical reaction of NO and superoxides, however, cause barrier dysfunction in the gastrointestinal mucosa (Greenacre *et al.* 1997; Unno *et al.* 1997). Thus, the effect of iNOS-produced NO on mucosal health in the stomach is particularly controversial.

Many investigators have examined the roles of iNOS-produced NO using iNOS inhibitors. The specificity and dose of iNOS inhibitor, however, are critical in such studies because no known inhibitor is completely selective for iNOS and most iNOS inhibitors may also inhibit constitutive NOS, which plays important roles in the maintenance of gastric mucosa integrity. Moreover, these inhibitors may have additional pharmacological effects that are not related to the NO pathway. In addition, these agents are difficult to administer continuously in living animals. These concerns may be responsible for the conflicting results that have been obtained by studies investigating the roles of iNOS in the gastric mucosa.

The processes of ulcer development and healing in experimental ulcer models have been well characterized (Halter *et al.* 1995), and striking similarities have been noted, regardless of the method of ulcer induction or the species of experimental animal (Halter *et al.* 1995; Schmassmann *et al.* 1995). In the present study, we examined the characteristics of iNOS expression during ulcer development and healing in the rat and mouse stomach and investigated the impact of *iNOS* gene deficiency on these processes in the mouse stomach.

Materials and methods

Rat experiments

Ulcer induction Animals were given free access to water and food during these experiments (CE-2, CLEA, Tokyo, Japan). Gastric ulcers were induced in male Wistar rats, weighing 220–250 g, according to the method described by Nakamura (Nakamura *et al.* 1995), with slight modifications. Briefly, anaesthesia was induced intraperitoneally in the experimental animal using pentobarbital

(1 mg/kg). One hundred per cent acetic acid was then applied to the serosal surface of the antrum–corpus junction of the anterior wall of the rat stomach for 40 s using a plastic mould with an inner diameter of 5 mm. After washing out the acetic acid with saline solution, the abdominal wall was closed.

Rats were killed using an overdose of ether at 24, 36, 48 and 72 h and at 7 and 14 days after ulcer induction. The stomachs were removed, opened along the greater curvature and spread out. The ulcerous portions of the tissues were then excised; some portions were immediately frozen in liquid nitrogen to be used in the iNOS mRNA expression analyses, while others were fixed for 12 h with 10% buffered formaldehyde (pH 7.4) and used for histological examination.

RNA preparation and Northern blot analysis Total RNA was isolated from the frozen tissues using the guanidine thiocyanate extraction method (Chomczynski & Sacchi 1987). Twenty micrograms of total RNA was then electrophoresed on a 1% agarose gel containing 6% formaldehyde and then transferred to a Hybond-N membrane (Amersham Pharmacia Biotech, Uppsala, Sweden). After ultraviolet cross-linking, the filter was prehybridized and hybridized as described previously (Fujisawa *et al.* 1995). A 0.7 kb fragment of rat cDNA (-190 to 424, gene bank index, 31377499) (Adachi *et al.* 1993) was then labelled with [α-^{32}P]dCTP (3000 Ci/mmol) using a random priming kit (Amersham Pharmacia Biotech). The filter was washed four times at 58 °C in $2\times$ saline sodium citrate (SSC; $1\times$ SSC: 0.15 M NaCl and 1.5 mM sodium citrate) per 0.1% SDS containing 0.2% sodium pyrophosphate and then exposed to an imaging plate. The radioactivity was then analysed using a Bio-image analyser BAS 2000 (Fuji Photo Film Co., Tokyo, Japan). To evaluate the amount of RNA analysed, the filter was rehybridized with a ^{32}P-labelled cDNA probe for rat β-actin containing the entire coding region (Tokunaga *et al.* 1986).

Histochemical study After tissue fixation, paraffin sections were routinely prepared. Deparaffinized sections were washed with phosphate-buffered saline (PBS) and autoclaved at 120 °C for 10 min in a 10 mM citrate buffer (pH 6.0), as described previously (Ehara *et al.* 1996). Endogenous peroxide activity was blocked by incubating with 0.3% H_2O_2 in methanol, and the sections were treated with 10% normal goat serum in PBS. The sections were then reacted with rabbit serum immunized against the rat iNOS protein (Ohshima *et al.* 1992) (dilution 1 : 1000) in PBS containing 1% bovine serum albumin. The sections were secondarily reacted with biotinylated anti-rabbit immunoglobulin G goat serum, and an avidin–biotin–immunoperoxidase complex was formed

using a Dako LSAB kit (DAKO Corporation, Carpinteria, CA, USA). iNOS protein was detected using 3,3′-diaminobenzidine tetrahydrochloride in 50 mм Tris–HCl (pH 7.6). The nuclei were counterstained with haematoxylin. The same procedure minus the primary antibody reaction was performed as a negative control.

iNOS$^{-/-}$ mice experiments

Ulcer induction. C57BL/6-iNOS$^{-/-}$ mice were obtained from the Jackson Laboratory (Bar Harbor, ME, USA) (Laubach *et al*. 1995). Wildtype C57BL/6 mice were obtained from Charles River Japan Inc. (Kanagawa, Japan) and used as controls. All mice were male, 8–10 weeks old, and weighed 18–24 g. Gastric ulcers were induced in the mice using a modification of a previously described cryoinjury method (Inauen *et al*. 1988). Briefly, animals that had been fed after undergoing a 24 h fast were anaesthetized using an intraperitoneal injection of 2-2-2 tribromoethanol (0.28 mg/g), and a median laparotomy was performed. A freezing injury was induced on the serosal surface of the ventral wall of the antrum–corpus junction by applying a cryoprobe (cooled using gaseous CO_2) with a diameter of 3 mm to the gastric wall for 15 s. The abdomen was then closed using silk sutures.

Wildtype and iNOS$^{-/-}$ mice were killed using an overdose of ether at 1, 3, 5, 7 and 14 days after ulcer induction. The stomach was then opened along the greater curvature and pinned to a board so that the stomach was slightly stretched. The ulcer lesion was then photographed using a digital still camera (MVC-FD7; Sony, Tokyo, Japan), and RNA and histological sections of the stomachs were prepared as described above.

Reverse-transcriptase-polymerase chain reaction. Single-strand cDNA was synthesized using a commercial kit in a reaction volume of 15 μl containing 5 μg of total RNA and 0.2 μg of random hexamer primers, according to the kit manufacturer's instructions (Pharmacia P-L Biochemicals, Milwaukee, WI, USA). To detect mouse iNOS and β-actin mRNA, 0.3 μl of single-strand cDNA was amplified by polymerase chain reaction (PCR) using the following oligonucleotide primers: mouse iNOS, 5′-TGCATGGACCAGTATAAGGCAAGC-3′ and 5′-GCTTCTGGTCGATGTCATGAGCAA-3′ (Lyons *et al*. 1992); β-actin, 5′-GCCAGGTCATCACTATT-GGC-3′ and 5′-TCAAGTCAGTGTACAGGGCCA-3′. Denaturation, annealing and elongation were performed at 94, 55 and 72 °C for 30 s, 1 min and 2 min, respectively, for 35 cycles for iNOS and 28 cycles for β-actin. Next, 8 μl of each PCR product was separated on

a 2% agarose gel, stained with 0.5 μg/ml of ethidium bromide and photographed.

Measurement of ulcer size The ulcer area was measured on macroscopic digital photographs using an image analysis program (NIH Image, Version 1.58). In addition, sections from the middle portion of each ulcer were stained with haematoxylin and eosin (H&E), photographed under a microscope (original magnification, ×100) and digitized into 1074 × 756 pixels using a digitizer (N-20; Nikon, Tokyo, Japan). The thickness of the injured epithelium region was measured in each section using the above-mentioned image analysis program running on a personal computer.

Detection of proliferating cells, vessel counting and apoptotic cells. Proliferating cells were detected by labelling newly synthesized DNA using the BrdU-incorporation method, as previously described (Yamashita *et al*. 1994). The number of stained cells in the proliferation zone was then counted.

Endothelial cells were stained using anti-CD31 antibody (Pharmingen International, San Diego, CA, USA). The microvascular density of the granulation tissue or submucosa at the middle portion of the ulcer was then measured. Individual microvessel counts were made using a ×100 field. Any brownish red-staining endothelial cells or endothelial clusters, with or without a lumen, which were clearly separate from adjacent microvessels were considered to be single and countable microvessels.

Apoptotic cells were immunohistochemically detected using the *in situ* cell death detection kit, ApopTag™ (Intergen Company, Purchase, NY, USA) and the terminal deoxyuridine nucleotidyl nick end labelling method, according to the manufacturer's protocol. The number of stained cells visible on a printed photograph was then counted using a blind study design.

Results

iNOS expression in acetic acid-induced rat ulcers

Gastric ulcers appeared in the rats 24–48 h after ulcer induction. The whitish necrotic tissue had nearly disappeared from the ulcer bed 14–16 days after the acetic acid treatment. During the ulceration and healing processes, iNOS mRNA was detected in the stomach at 24 h, peaking at 72 h (3 days) after acetic acid treatment (Figure 1). The time course for the appearance of iNOS-positive cells was also examined immunohistochemically in the rat stomach after acetic acid treatment (Figure 2). iNOS-positive inflammatory cells infiltrated the damaged lamina propria from the intact submucosa at 24 h after
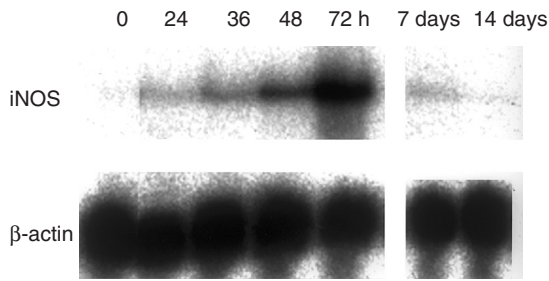
Figure 1. Time course for the expression of inducible nitric oxide synthase (iNOS) mRNA after ulcer induction in the rat stomach. Ulcers were induced using 100% acetic acid. The expression of iNOS mRNA was analysed using Northern blotting.

ulcer induction (arrow head) (Figure 2b). Submucosal oedema was observed during the period of ulcer development, but, the number of iNOS-positive cells was small (Figure 2b). During the early healing process, the number of iNOS-positive cells increased, but these cells were only found distributed in the ulcer bed in the gastric mucosa at 72 h after ulcer induction (Figure 2c). The iNOS-positive cells were detected among inflammatory cells and fibroblasts (Figure 2d). Once the oedema
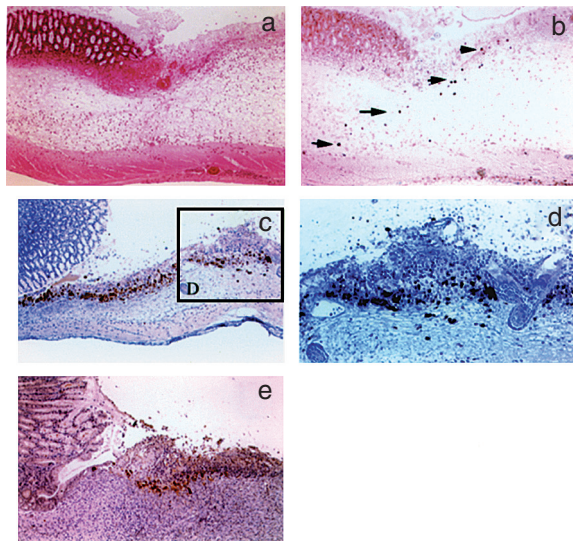

Figure 2. Localization of inducible nitric oxide synthase (iNOS) protein in acetic acid-induced gastric rat ulcers. The localization of rat iNOS-positive cells after ulcer induction using acetic acid was immunohistochemically examined. (a) Haematoxylin and eosin staining of a specimen obtained 24 h after ulcer induction. (b) iNOS immunostaining of specimens obtained 24 h after ulcer induction, (c) 72 h after ulcer induction and (e) 7 days after ulcer induction. (d) Higher magnification of the specimen shown in c (original magnification of a, b, c and e, ×100; d, ×200). Arrows indicate iNOS-positive cells.

had decreased, the number of iNOS-positive cells dramatically increased (Figure 2c). During the healing process, iNOS-positive cells were observed in areas lacking re-epithelialization in the ulcer bed, and the number of iNOS-positive cells declined as the ulcer bed re-epithelialized over the 7 days following ulcer induction (Figure 2e).

Time course change in iNOS mRNA expression and histological appearances in cryoinjury-induced mice ulcers

The expression of iNOS mRNA was observed in the mice stomachs using reverse transcriptase-PCR on days 3–7 after ulcer induction (Figure 3).

Although the time course changes in the histological appearance of the cryoinjury-induced mice ulcers were delayed by 2–3 days, compared to the day of peak inflammation in the ulcer beds of the acetic acid-induced rat ulcers, the subsequent healing course was similar in mice and rats. Figure 4 shows microphotographs of H&E-stained sections from wildtype mice (a, b, c, d and e) and iNOS$^{-/-}$ mice (f, g, h, i and j). Photographs (a) and (f), (b) and (g), (c) and (h), (d) and (i) and (e) and (j) indicate the histological appearance on days 1, 3, 5, 7 and 14 after ulcer induction, respectively. No significant differences in histological appearance were observed between wildtype and iNOS$^{-/-}$ mice until 3 days after ulcer induction. The thickness of the submucosa during this period indicates the degree of mucosal oedema. No significant difference in the thickness of the ulcer bed was seen between the iNOS$^{-/-}$ mice and the wildtype mice (0.66 ± 0.14 mm *vs.* 0.62 ± 0.06 mm, respectively; $n = 6$, $P = 0.542$) at 3 days after ulcer induction. However, the degree of inflammation in the ulcer beds of the iNOS$^{-/-}$ mice 7 days after ulcer induction was more severe than that of the wildtype mice (Figure 4-d *vs.* i).
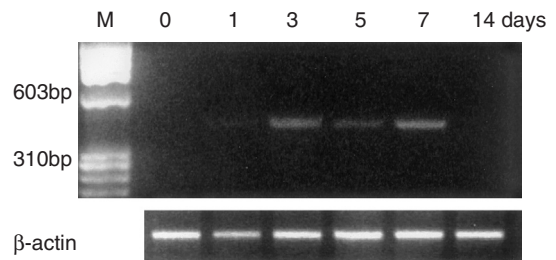
Figure 3. Time course of inducible nitric oxide synthase (iNOS) mRNA expression in wildtype mice. Ulcers were induced by cryoinjury in the mice stomachs. iNOS mRNA expression was examined using reverse transcriptase-polymerase chain reaction.
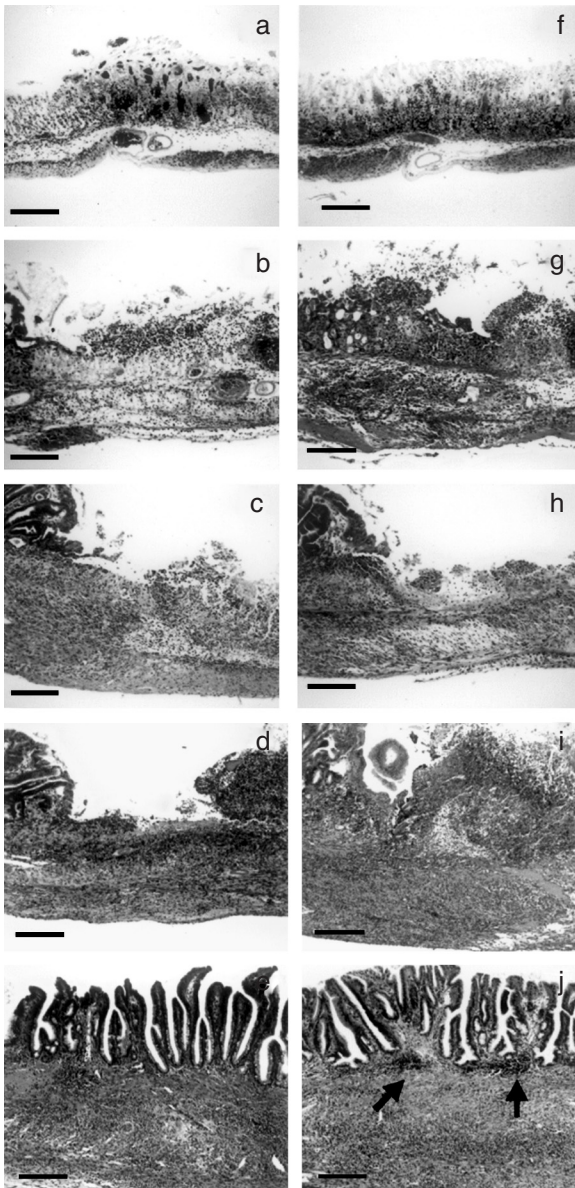
Figure 4. Comparison of the microscopic appearances of cryoinjury-induced gastric ulcers in inducible nitric oxide synthase (iNOS$^{-/-}$) and wildtype mice. The microphotographs show haematoxylin and eosin-stained specimens from wildtype mice (a, b, c, d and e) and iNOS$^{-/-}$ mice (f, g, h, i and j): (a) and (f), day 1; (b) and (g), day 3; (c) and (h), day 5; (d) and (i), day 7; (e) and (j), day 14 after ulcer induction. Aggregates of mononuclear cells in the submucosa (arrow heads) were frequently seen in specimens from iNOS$^{-/-}$ mice obtained 14 days after ulcer induction (j). Bar, 100 μm.

The ulcer bed at 7 days after ulcer induction was filled with inflammatory cells; thus, the thickness of the ulcer bed indicates the degree of inflammation. The mean thickness of the ulcer bed in the iNOS$^{-/-}$ mice was significantly higher than that in the wildtype mice (1.51 ± 0.15 mm *vs.* 0.98 ± 0.22 mm, respectively; $n = 7$, $P < 0.01$). Aggregates of mononuclear cells in the submucosa were frequently seen in specimens obtained from iNOS$^{-/-}$ mice 14 days after ulcer induction (Figure 4e).

The area of the ulcers was quantitatively compared between wildtype and iNOS$^{-/-}$ mice on days 1, 3, 5, 7 and 14 (Figure 5). The mean ulcer area in iNOS$^{-/-}$ mice 5 days after ulcer induction was significantly ($P < 0.05$) larger than that in wildtype mice.

Proliferating cells, vessel formation and apoptotic cells during the ulcer healing process

Time course changes in the number of BrdU-incorporated epithelial cells, newly formed vessels and apoptotic cells are shown in Figure 6. No differences in the number of stained cells in the proliferation zone (healing zone) or the number of vessels stained by the anti-CD31 antibody were seen between wildtype and iNOS$^{-/-}$ mice throughout the time course of the present study (Figure 6a,b). Although the number of apoptotic cells in the granulation tissue was not different between wildtype and iNOS$^{-/-}$ mice until 7 days after ulcer induction, the number of apoptotic cells in the submucosal area under the new epithelium 14 days after ulcer induction had dramatically increased in the wildtype mice, but not in the iNOS$^{-/-}$ mice (Figure 6c,d) ($n = 6-9$).
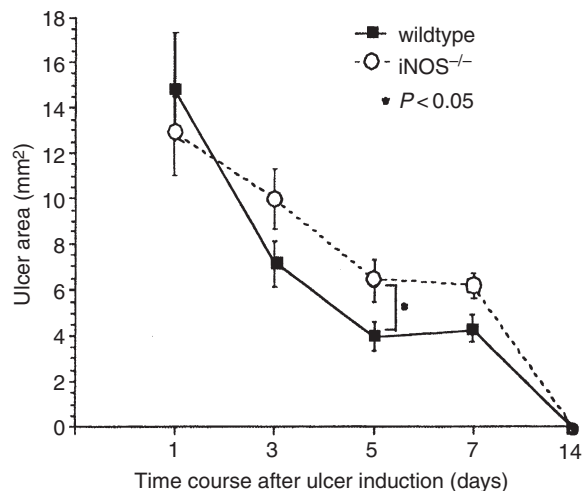
Figure 5. Time course changes in ulcer area. Ulcer area was measured using an image analysis program running on a personal computer. Results are shown as the mean ± SE ($n = 6-9$).
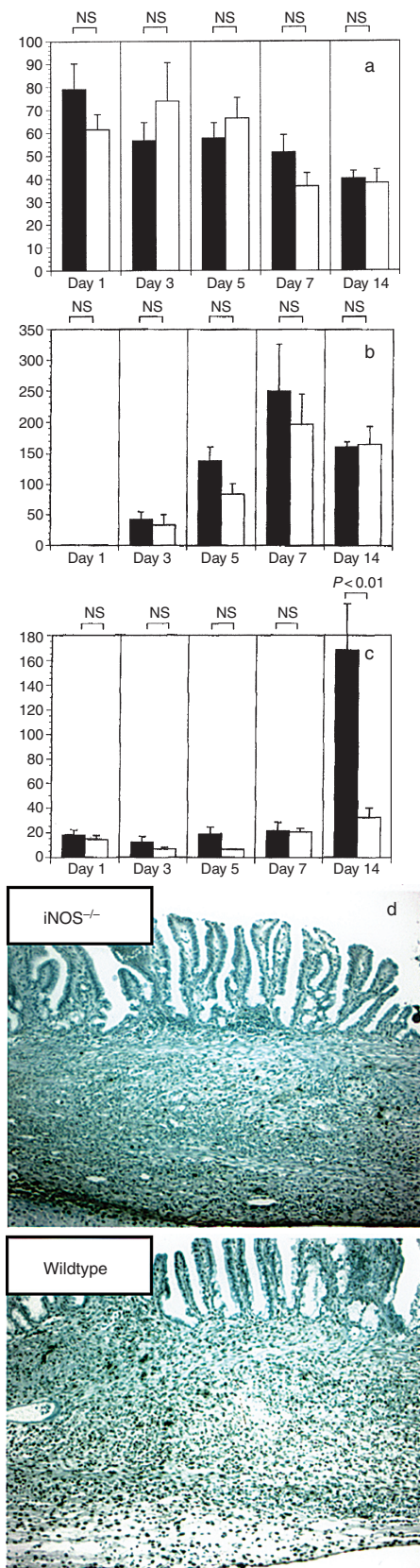
Discussion

The processes of ulcer development and healing in experimental ulcer models have been similarly classified into an ulcer development phase (days 0–1) and four healing phases: an early lag phase (days 1–3), a rapid healing phase (days 3–14), a late lag phase (days 14–18) and a remodelling phase (day 18 and onward) (Halter *et al*. 1995). In this study, we examined the ulceration and healing processes in both rats and mice. Although the early lag phase in the cryoinjury-induced mice ulcers was longer than that in the acetic acid-induced rat ulcers, iNOS expression was well correlated with the histological stage of ulcer healing, independent of species. Namely, iNOS mRNA expression was first detected in the early lag phase, after mucosal necrosis and the exfoliation of the necrotic tissue, and peaked as the rapid healing phase began (Halter *et al*. 1995).

The time course for the appearance of iNOS-positive cells was also examined immunohistochemically in the acetic acid-induced rat ulcers. iNOS-positive cells were observed during the rapid healing phase in areas of the ulcer bed that lacked re-epithelialization; the number of iNOS-positive cells then declined as the ulcer bed re-epithelialized over the 7 days following ulcer induction. These observations, as well as the time course of iNOS mRNA expression in induced ulcers, indicate that iNOS-produced NO may be involved in the formation of necrotic regions, where the damaged mucosa is detached into the gastric lumen. This process plays an important role in ulcer healing, because a gelatinous coat covering the ulcer bed and consisting of a fibrin-based gel with mucus and necrotic cells acts to protect the ulcer bed by preventing direct contact with the gastric luminal contents, such as gastric acid, pepsin and ingested foods (Allen *et al*. 1988).

Clarifying whether iNOS has a detrimental or beneficial effect on the process of ulcer development and healing is of great interest to researchers. In this study,

Figure 6. Time course changes in the number of proliferating cells, newly formed vessels and apoptotic cells in the granulation tissue of gastric mouse ulcers. Proliferating cells were detected by labelling newly synthesized DNA using the BrdU-incorporation method. Vessel formation and apoptotic cells were immunohistochemically detected using an anti-CD31 antibody and the terminal deoxyuridine nucleotidyl nick end labelling (TUNEL) method, respectively. The number of stained cells in the granulation tissue of the ulcer bed and the submucosal area after re-epithelization was counted. (a) BrdU incorporation. (b) Vessel number. (c) TUNEL staining. Results are shown as the mean ± SE ($n=6–9$). ■, wildtype mice; □, iNOS$^{-/-}$ mice. (d) Microphotograph of TUNEL staining in specimens obtained 14 days after ulcer induction (original magnification, ×100).

we obtained important information on the histological characteristics of iNOS-positive cells, including the time course for their appearance, their cellular origins and their distribution in ulcer tissues. Oedema formation in the gastrointestinal mucosa is reportedly exacerbated by NO produced as a result of iNOS activity (Salvemini *et al.* 1996). In the present study, submucosal oedema was observed during the period of ulcer development, but the number of iNOS-positive cells was small. Once the oedema had decreased, the number of iNOS-positive cells increased dramatically. These findings suggest that the mucosal oedema did not form as a result of iNOS activity during ulcer progression. Moreover, no significant difference in oedema formation was observed between wildtype and iNOS$^{-/-}$ mice in the present study. In addition, the maximum ulcer size after ulcer induction did not differ between wildtype and iNOS$^{-/-}$ mice, suggesting that iNOS activity was not involved in ulcer progression. An earlier study demonstrated a positive association between iNOS expression and colitis activity, with iNOS being induced in inflamed colonic epithelium (Singer *et al.* 1996). Thus, the cellular origin of iNOS may determine whether NO has a beneficial or detrimental effect on mucosal health. If iNOS were to act detrimentally on ulcer healing and development, iNOS would be expressed in the ulcer margin, which is an important area for ulcer healing, supplying new epithelial cells (healing zone) (Tarnawski & Halter 1995). In this study, iNOS-positive cells were localized only among the inflammatory cells and fibroblasts. In addition, iNOS-positive cells were confined to an area between the necrotic tissues and the granulation tissues in the ulcer bed but were not found at the ulcer margin. This distribution pattern for iNOS-positive cells, likely covering the epithelium defect, may serve as a barrier against various pathogens.

In this study, the roles of iNOS in ulcer healing were considered from two perspectives: (1) re-epithelization or the period during which the mucosa is re-epithelized after ulcer induction and (2) the quality of ulcer healing. A previous study reported that a non-specific NOS inhibitor, N^G-nitro-L-arginine, delays ulcer healing (Brzozowski *et al.* 1995). Furthermore, Akiba *et al.* (1998) demonstrated that the oral administration of aminoguanidine, a relatively specific iNOS inhibitor, delayed ulcer healing in the same experimental rat ulcer model that was used in the present study. However, whether the delay in ulcer healing might be due to the inhibition of constitutive NOS (which plays an important role in the maintenance of mucosal integrity) but not of iNOS or to some other effect of the inhibitor was not addressed in these studies. In the present study, the period during which the mucosa was re-epithelized did not differ between iNOS$^{-/-}$ and wildtype mice. However, the mean ulcer size in the iNOS$^{-/-}$ mice was larger than that in wildtype mice 5 days after ulcer induction. This result is consistent with the findings of a skin ulcer model using iNOS$^{-/-}$ mice (Yamasaki *et al.* 1998). The inflammatory response in iNOS$^{-/-}$ mice 7 days after ulcer induction was severer than that in wildtype mice. At 14 days after ulcer induction, the number of apoptotic cells amongst the neutrophils and mononuclear cells infiltrating the subepithelial mucosa of wildtype mice dramatically increased, but this phenomenon was not seen in iNOS$^{-/-}$ mice. Furthermore, aggregates of mononuclear cells were found in the subepithelium of specimens from iNOS$^{-/-}$ mice. These results indicate that inflammation in the granulation tissue was prolonged in the iNOS$^{-/-}$ mice. Hickey *et al.* (1997) reported that iNOS activity regulates leucocyte recruitment, by affecting the expression of adhesion molecules or leucocyte activation. The regulation of inflammation during the healing phase (3 days after ulcer induction) and up until the remodelling phase is a key process because the persistent infiltration of polymorphonuclear cells is the most prominent factor in gastric ulcer scarring in rats, which predisposes them to ulcer recurrence (Arakawa *et al.* 1998). Recent clinical findings also suggest a close relationship among the quality of ulcer healing, the infiltration of neutrophils and mononuclear cells and future ulcer recurrence (Nebiki *et al.* 1997). These results indicate that iNOS gene expression might regulate inflammatory responses during ulcer healing and, consequently, play an important role in the quality of ulcer healing.

In this study, no difference in re-epithelization or angiogenesis was seen in the ulcer beds of the iNOS$^{-/-}$ and wildtype mice. However, further studies are needed to confirm that iNOS activity was not involved in the phenomenon, as compensatory reactions to the functional loss of the iNOS gene must be taken into consideration. The upregulation of eNOS and transforming growth factor-β1 was recently demonstrated in iNOS$^{-/-}$ mice using a skin incision wound model, suggesting that alternate healing pathways may occur in response to a lack of functional iNOS (Most *et al.* 2002). On the other hand, the downregulation of bFGF and interleukin-4 was also seen in iNOS$^{-/-}$ mice in the above study. Thus, numerous complicated mechanisms are probably involved in the process of ulcer healing. The comprehensive identification of growth factors associated with ulcer healing using, for example, gene-chip techniques may be required to precisely understand the roles of iNOS activity in re-epithelization.

In conclusion, we have characterized iNOS expression during the development and healing of experimentally induced ulcers in rats and mice. Our findings suggest that iNOS activity affects the regulation of inflammatory responses during ulcer healing, playing a beneficial role in ulcer healing.

References

ADACHI H., IIDA S., OGUCHI S. *ET AL.* (1993) Molecular cloning of a cDNA encoding an inducible calmodulin-dependent nitric-oxide synthase from rat liver and its expression in COS1 cells. *Eur. J. Biochem.* **217**, 37–43.

AKIBA Y., NAKAMURA M., MORI M. *ET AL.* (1998) Inhibition of inducible nitric oxide synthase delays gastric ulcer healing in the rat. *J. Clin. Gastroenterol.* **27**, S64–S73.

ALLEN A., LEONARD A.J. & SELLERS L.A. (1988) The mucus barrier. Its role in gastroduodenal mucosal protection. *J. Clin. Gastroenterol.* **10**, S93–S98.

ARAKAWA T., WATANABE T., FUKUDA T. *ET AL.* (1998) Ulcer recurrence: cytokines and inflammatory response-dependent process. *Dig. Dis. Sci.* **43**, 61S–66S.

BRZOZOWSKI T., KONTUREK S.J., DROZDOWICZ D., DEMBINSKI A. & STACHURA J. (1995) Healing of chronic gastric ulcerations by 1-arginine. Role of nitric oxide, prostaglandins, gastrin and polyamines. *Digestion* **56**, 463–471.

CHOMCZYNSKI P. & SACCHI N. (1987) Single-step method of RNA isolation by acid guanidinium thiocyanate–phenol–chloroform extraction. *Anal. Biochem.* **162**, 156–159.

EHARA H., DEGUCHI T., KOJI T. *ET AL.* (1996) Autoclave antigen retrieval technique for immunohistochemical staining of androgen receptor in formalin-fixed paraffin sections. *Acta. Histochem. Cytochem.* **29**, 311–318.

FUJISAWA H., OGURA T., HOKARI A., WEISZ A., YAMASHITA J. & ESUMI H. (1995) Inducible nitric oxide synthase in a human glioblastoma cell line. *J. Neurochem.* **64**, 85–91.

GREENACRE S., RIDGER V., WILSONCROFT P. & BRAIN S.D. (1997) Peroxynitrite: a mediator of increased microvascular permeability? *Clin. Exp. Pharmacol. Physiol.* **24**, 880–882.

HALTER F., SCHMASSMANN A. & TARNAWSKI A. (1995) Healing of experimental gastric ulcers. *Dig. Dis. Sci.* **40**, 2481–2486.

INAUEN W., WYSS P.A., KAYSER S. *ET AL.* (1988) Influence of prostaglandins, omeprazole, and indomethacin on healing of experimental gastric ulcers in the rat. *Gastroenterology* **95**, 636–641.

KUBES P., SUSUKI M. & GRANGER D. (1991) Nitric oxide: An endogenous modulator of leukocyte adhesion. *PNAS* **88**, 4651–4655.

LAUBACH V.E., SHESELY E.G., SMITHIES O. & SHERMAN P.A. (1995) Mice lacking inducible nitric oxide synthase are not resistant to lipopolysaccharide-induced death. *Proc. Natl. Acad. Sci. USA* **92**, 10688–10692.

LYONS C.R., ORLOFF G.J. & CUNNINGHAM J.M. (1992) Molecular cloning and functional expression of an inducible nitric oxide synthase from a murine macrophage cell line. *J. Biol. Chem.* **267**, 6370–6374.

McCAFFERTY D.M., MUDGETT J.S., SWAIN M.G. & KUBES P. (1997) Inducible nitric oxide synthase plays a critical role in resolving intestinal inflammation. *Gastroenterology* **112**, 1022–1027.

MOST D., EFRON D.T., SHI H.P., TANTRY U.S. & BARBUL A. (2002) Characterization of incisional wound healing in inducible nitric oxide synthase knockout mice. *Surgery* **132**, 866–876.

NAKAMURA M., ODA M., INOUE J. *ET AL.* (1995) Plasticity of myofibroblasts appearing in granulation tissues after acetic acid treatment. Effect of bFGF. *Dig. Dis. Sci.* **40**, 2477–2480.

NEBIKI H., ARAKAWA T., HIGUCHI K. & KOBAYASHI K. (1997) Quality of ulcer healing influences the relapse of gastric ulcers in humans. *J. Gastroenterol. Hepatol.* **12**, 109–114.

OHSHIMA H., BROUET I., BABDALETOVA T. *ET AL.* (1992) Polyclonal antibody against an inducible form of nitric oxide synthase purified from the liver of rats treated with *Propionibacterium acnes* and lipopolysaccharide. *Biochem. Biophys. Res. Commun.* **187**, 1291–1297.

SALVEMINI D., WANG Z.Q., WYATT P.S. *ET AL.* (1996) Nitric oxide: a key mediator in the early and late phase of carrageenan-induced rat paw inflammation. *Br. J. Pharmacol.* **118**, 829–838.

SALZMAN A., EAVES-PYLES T., LINN S., DENENBERG A. & SZABO C. (1998) Bacterial induction of inducible nitric oxide synthase in cultured human intestinal epithelial cells. *Gastroenterology* **114**, 93–102.

SCHMASSMANN A., TARNAWSKI A., PESKAR B.M., VARGA L., FLOGERZI B. & HALTER F. (1995) Influence of acid and angiogenesis on kinetics of gastric ulcer healing in rats: interaction with indomethacin. *Am. J. Physiol.* **268**, G276–G285.

SINGER I.I., KAWKA D.W., SCOTT S. *ET AL.* (1996) Expression of inducible nitric oxide synthase and nitrotyrosine in colonic epithelium in inflammatory bowel disease. *Gastroenterology* **111**, 871–885.

TARNAWSKI A. & HALTER F. (1995) Cellular mechanisms, interactions, and dynamics of gastric ulcer healing. *J. Clin. Gastroenterol.* **21**, S93–S97.

TOKUNAGA K., TANIGUCHI H., YODA K., SHIMIZU M. & SAKIYAMA S. (1986) Nucleotide sequence of a full-length cDNA for mouse cytoskeletal beta-actin mRNA. *Nucleic Acids Res.* **14**, 2829.

UNNO N., WANG H., MENCONI M.J. *ET AL.* (1997) Inhibition of inducible nitric oxide synthase ameliorates endotoxin-induced gut mucosal barrier dysfunction in rats. *Clin. Exp. Pharmacol. Physiol.* **24**, 1246–1257.

YAMASAKI K., EDINGTON H.D., McCLOSKY C. *ET AL.* (1998) Reversal of impaired wound repair in iNOS-deficient mice by topical adenoviral-mediated iNOS gene transfer. *J. Clin. Invest.* **101**, 967–971.

YAMASHITA N., MINAMOTO T., ONDA M. & ESUMI H. (1994) Increased cell proliferation of azoxymethane-induced aberrant crypt foci of rat colon. *Jpn. J. Cancer Res.* **85**, 692–698.